Follow us @BoneJointRes

Freely available online OPEN ACCESS

BJR

BONE FRACTURE

Fibrinolysis as a target to enhance osteoporotic fracture healing by vibration therapy in a metaphyseal fracture model

R. M. Y. Wong,
V. M. H. Choy,
J. Li,
T. K. Li,
Y. N. Chim,
M. C. M. Li,
J. C. Y. Cheng,
K-S. Leung,
S. K-H. Chow,
W. H. Cheung

From The Chinese University of Hong Kong, Hong Kong Special Administrative Region, The People's Republic of China

Aims

Fibrinolysis plays a key transition step from haematoma formation to angiogenesis and fracture healing. Low-magnitude high-frequency vibration (LMHFV) is a non-invasive biophysical modality proven to enhance fibrinolytic factors. This study investigates the effect of LMHFV on fibrinolysis in a clinically relevant animal model to accelerate osteoporotic fracture healing.

Methods

A total of 144 rats were randomized to four groups: sham control; sham and LMHFV; ovariectomized (OVX); and ovariectomized and LMHFV (OVX-VT). Fibrinolytic potential was evaluated by quantifying fibrin, tissue plasminogen activator (tPA), and plasminogen activator inhibitor-1 (PAI-1) along with healing outcomes at three days, one week, two weeks, and six weeks post-fracture.

Results

All rats achieved healing, and x-ray relative radiopacity for OVX-VT was significantly higher compared to OVX at week 2. Martius Scarlet Blue (MSB) staining revealed a significant decrease of fibrin content in the callus in OVX-VT compared with OVX on day 3 ($p = 0.020$). Mean tPA from muscle was significantly higher for OVX-VT compared to OVX ($p = 0.020$) on day 3. Mechanical testing revealed the mean energy to failure was significantly higher for OVX-VT at 37.6 N mm (SD 8.4) and 71.9 N mm (SD 30.7) compared with OVX at 5.76 N mm (SD 7.1) ($p = 0.010$) and 17.7 N mm (SD 11.5) ($p = 0.030$) at week 2 and week 6, respectively.

Conclusion

Metaphyseal fracture healing is enhanced by LMHFV, and one of the important molecular pathways it acts on is fibrinolysis. LMHFV is a promising intervention for osteoporotic metaphyseal fracture healing. The improved mechanical properties, acceleration of fracture healing, and safety justify its role into translation to future clinical studies.

Cite this article: *Bone Joint Res* 2021;10(1):41–50.

Keywords: Fibrinolysis, Vibration therapy, Osteoporotic fracture, Metaphyseal fracture, LMHFV

Article focus

- Fibrinolysis is suggested by recent evidence to be a key transition stage between haematoma formation and angiogenesis during fracture healing, and thus is critical to the success of bone healing.
- Low-magnitude high-frequency vibration (LMHFV) is a biophysical intervention that has previously been shown to be effective in accelerating osteoporotic fracture healing.
- It is hypothesized that vibration therapy can enhance fibrinolysis and accelerate the transition from the haematoma formation to the angiogenesis phase of the healing process in an osteoporotic metaphyseal fracture animal model.

Correspondence should be sent to Wing Hoi Cheung; email: louischeung@cuhk.edu.hk

doi: 10.1302/2046-3758.101.BJR-2020-0185.R1

Bone Joint Res 2021;10(1):41–50.

Key messages

- Fibrinolysis potential was shown to be impaired or delayed in an ovariectomy-induced osteoporotic fracture model at the metaphyseal region with higher fibrin content during the transition stage.
- Vibration treatment significantly decreased fibrin contents at the metaphyseal fracture site that is accompanied with the increased detected signals of tissue plasminogen activator (tPa), decreased signals of plasminogen activator inhibitor-1 (PAI-1), and eventually better mechanical outcome.

Strengths and limitations

- This is the first study to investigate the role of fibrinolysis during fracture healing in a clinically relevant osteoporotic fracture animal model at the metaphyseal region that heals primarily through intramembranous ossification.
- The findings of this animal study may need to be verified in human studies.

Introduction

Osteoporosis predisposes patients to increased risk of fragility fractures and approximately 2.5 million osteoporotic fractures occur each year in the USA, with costs projecting to $25 billion USD by 2025.[1] In fact, the disease has become a worldwide threat, with the lifetime fracture risk of osteoporotic patients reaching as high as 40%.[2,3] It is well known that most osteoporotic fractures occur at the metaphyseal regions of long bones, including the distal radius, proximal humerus, or proximal femur.[3-5] Therefore, it is now recommended that scientific studies should concentrate in these regions, which focus on trabecular bone formation.[6]

To enhance osteoporotic fracture healing, novel intervention therapies including microRNA,[7] small interfering RNA (siRNA),[8] or various kinds of biomaterials have been identified to rescue bone loss and promote bone healing in preclinical studies.[9] More importantly, a recent study showed that fibrinolysis was critical to normal healing of fractures.[10] The long-standing concept of the haematoma clot being essential for mesenchymal stem cell recruitment and neovascularization has recently been challenged, in a study in which normal fracture healing was found to occur in mice incapable of making fibrinogen.[11] In fact, Yuasa et al[10] showed that fibrin was entirely dispensable and fibrin-containing cartilage caused by inefficient fibrinolysis failed to undergo primary bone formation and remodelling, leading to derangement in diaphyseal fracture repair on mice. The removal of fibrin proved to be essential for the initiation of vascular invasion and penetration of the cartilage callus.[10,11] Fibrin deposition was essential for the initial haemostasis only. Impaired fibrinolysis is linked to osteoporosis and increased fracture risk.[12] There is currently convincing evidence that premenopausal women have greater fibrinolytic potential with lower tissue activator inhibitor-1 levels as compared to postmenopausal women.[13] Furthermore, postmenopausal women have significantly higher fibrinogen concentrations.[14] These studies demonstrate that oestrogen deficiency is strongly associated with decreased fibrinolytic potential. Further studies that target fibrinolysis to improve fracture healing in patients at risk are warranted.

Mechanical stimuli through physical exercise have been shown to prevent osteoporosis by mediating bone resorption and bone formation.[15] Low-magnitude high-frequency vibration (LMHFV) is a biophysical intervention that provides non-invasive, cyclic, and systemic mechanical stimulation.[16] Our previous studies have shown its positive effect in improving diaphyseal fracture healing, but it is still not proven for metaphyseal fractures, which is clinically relevant.[6,17] Vibration therapy improves fibrinolytic potential by increasing serum tissue plasminogen activator (tPA) concentrations in clinical patients.[18] Therefore, we hypothesize that vibration therapy can enhance fibrinolysis and accelerate the transition to the next phase of fracture healing. The aim of this study was to target fibrinolysis to enhance osteoporotic fracture healing and prove the effect of vibration therapy in an osteoporotic metaphyseal fracture model.

Methods

Experimental design and induction of osteoporosis. A total of 144 six-month-old female Sprague-Dawley rats were obtained from Laboratory Animal Services Centre of The Chinese University of Hong Kong (LASEC, CUHK) with approval from the animal ethics committee (Ref: 16 to 037-MIS). All rats were randomized to four groups: sham metaphyseal fracture (Sham; n = 36), sham metaphyseal fracture with LMHFV (Sham-VT; n = 36), ovariectomized metaphyseal fracture (OVX; n = 36), and ovariectomized metaphyseal fracture with LMHFV (OVX-VT; n = 36). Both OVX and OVX-VT rats underwent bilateral ovariectomy (OVX), and Sham and Sham-VT underwent sham operation under general anaesthesia as per our previously established protocols.[19] The rats were left for three months for establishment of osteoporosis, and bone mineral density (BMD) was measured to confirm that it had developed.[19]

Osteoporotic metaphyseal fracture model. After confirming the status of osteoporosis, all rats underwent a distal femur metaphyseal fracture as per our previously established protocol.[19] In brief, after general anaesthesia, the skin of left femur region was disinfected with povidone and draped in sterile towels. An incision was made along the lateral aspect of the distal femur. The vastus lateralis muscle and lateral head of the biceps femoris were split to expose the lateral condyle to the midshaft of the femur. A T-shaped mini-plate was used to fix the lateral femur with self-tapping screws. A small oscillating saw (OT7S-3, Piezosurgery Touch; Metron, Loreto, Italy) was

used to create an osteotomy just proximal to the epiphyseal cartilage at the metaphyseal region. The wound was irrigated with sterile normal saline and was closed in layers. Intramuscular buprenorphine (0.1/100 g; Schering-Plough, Kenilworth, New Jersey, USA) was given 15 minutes before surgery and three consecutive days after the procedure to minimize pain.

Intervention with low-magnitude high-frequency vibration. LMHFV was started the next day postoperatively for VT groups. A vibration platform (V-Health Ltd, Hong Kong, Hong Kong) that provided 35 Hz vertical vibration and a peak-to-peak magnitude of 0.3 g (g = gravitational acceleration) was used. The rats stood separately on a bottomless compartmented cage fixed on the vibration platform for 20 minutes per day, five days per week.[20] The rats in control groups were put on the platform with power off.

Specimen harvest. Rats were euthanized at three days, one week, two weeks, and six weeks post-fracture as complete healing was achieved at six weeks.[4] At three days, the haematoma clot is present and at one to two weeks it is in the bone formation phase. In order to detect fibrinolysis at the earliest stages of bone healing, the three days timepoint was selected.[21] During euthanasia, all rats were given an overdose of sodium pentobarbital (Hospira, Lake Forest, Illinois, USA). The left femur was harvested for micro-CT scanning.

Plain radiographs for fracture healing. Fracture healing was monitored by radiographs at endpoints according to established protocols.[19] Two independent surgeons (RMYW and KSL) assessed anteroposterior (AP) radiographs for fracture healing and lateral radiographs for cortical union. Metaphyseal fracture radiographs were further assessed and quantified by radiopacity in image analysis software (ImageJ; National Institutes of Health Bethesda, Maryland, USA).

Micro-CT analysis. Harvested femora were scanned by the micro-CT system (μCT-40; Scanco Medical, Brüttisellen, Switzerland). A small region of interest (ROI), 1.8 mm above and below the osteotomy site, was selected to avoid the diaphyseal region. Tissue volume (TV) was performed by semi-automatic contouring, and segmented with bone volume (BV). Microarchitectural parameters were evaluated by software provided by the manufacturer according to our previously established protocols.[20,22]

Fibrinolysis cytokine expression in fracture callus. After CT scan, expression of fibrinogen-related cytokines at the callus were quantified based on established protocols.[20] Formalin-fixed samples were decalcified, paraffin embedded, and sectioned at 5 μm thick. Histology sections were stained with haematoxylin and eosin (H&E) for general observation and Martius Scarlet Blue (MSB) stain for fibrin quantification. For immunohistochemistry (IHC), sections were subject to antigen retrieval in 60°C citrate buffer. Polyclonal primary antibodies of anti-tPA Tissue Plasminogen Activator antibody (ab14198; Abcam, Cambridge, UK), anti-PAI-1 antibody (ab66705; Abcam), anti-vascular endothelial growth factor (VEGF) (Sc-7269; Santa Cruz Biotechnology, Dallas, Texas, USA), and negative control buffer were applied overnight at 4°C. Images were captured under microscopy (Leica DMRB DAS; Leica, Heerbrugg, Switzerland) at 1.6 to 5 × objectives, and relative signals segmented by threshold in image analysis software (ImageJ) relative to negative control and expressed as mean positive signal area fraction per defined ROI at the callus.

Fibrinolysis cytokine expression in muscle. Approximately 5 mm^3 hamstring muscle samples were taken from areas without structural damage adjacent to the fracture site and harvested upon euthanasia. Specimens were immediately frozen with liquid nitrogen, crushed, and homogenized in a lysis solution (1% Triton X-100 in phosphate-buffered saline (PBS) at pH 7.4 mixed with cOmplete, EDTA-free Protease Inhibitor; Sigma-Aldrich, St. Louis, Missouri, USA). Using a vortex mixer, samples were incubated for 16 hours at 4°C with continuous shaking. Following centrifugation at 13,000 rpm, 4°C for ten minutes, the supernatants were collected, aliquoted, and stored at -80°C. The total protein concentration of the homogenate was determined using the Pierce BCA Protein Assay Kit (Thermo Fisher Scientific, Waltham, Massachusetts, USA). Then, tPa and PAI-1 concentrations of the supernatant were quantified using rat tPa ELISA Kit (ab198510; Abcam) and rat PAI-1 ELISA Kit (ab201283; Abcam).[23] The proteins of interest in hamstrings were calculated as concentration of target protein normalized by the ratio of total protein concentration among samples (ng/ml for tPa; pg/ml for PAI-1).

Fibrinolysis cytokines in serum. Blood was collected from the rats under anaesthesia by cardiac puncture before euthanasia and stored into serum separator tubes.[20] Blood was centrifuged at 1,500 g for 15 minutes at room temperature. Supernatant was collected and centrifuged again at 13,000 g for 15 minutes at room temperature. Serum was then stored at -80°C until assessment. Serum tPa (ab198510; Abcam) and PAI-1 (ab201283; Abcam) levels were detected by enzyme-linked immunosorbent assay (ELISA) kits. The concentrations of target proteins were determined and expressed as ng/ml for tPa; pg/ml for PAI-1.

Mechanical testing. Entire femora were dissected free from soft tissues with the metal implants removed. Each femur was mounted in a performance polymer testing jig[24] (Ureol 2020; Ciba, Hong Kong, Hong Kong) at the proximal end and fixed to the material testing machine (H25KS; Hounsfield Test Equipment, Redhill, UK) at 25° above the horizontal where the angle was chosen to mimic the in situ physiological loading conditions. A compressive force at the constant downward velocity of 25 mm per minute was applied by a metal blade at the epiphysis, directly above the second screw hole. The specimens were tested to failure and the load-displacement curves of the fractured femora were generated by the built-in software. The ultimate load (failure force) (N), stiffness (N/mm),

and the energy to failure (N mm) were recorded and analyzed using built-in software (QMAT Professional Material testing software; Tinius Olsen, Horsham, Pennsylvania, USA).[20] The failure force and the energy at failure were compared among different groups.

Statistical analysis. All quantitative data were expressed as mean and SD and analyzed with SPSS version 24.0 software (IBM, Armonk, New York, USA). One-way analysis of variance (ANOVA) with post-hoc Bonferroni test were used to compare the differences at different timepoints. Significant difference was set at a probability level of 95% ($p \leq 0.05$).

Results

Clinical results. All rats resumed weight-bearing as tolerated after the surgery. A total of 34 OVX rats (34/36 × 100% = 94%) and 35 OVX-VT rats (35/36 × 100% = 97%) survived the overall observation period, while 35 Sham rats (35/36 × 100% = 97%) and 34 Sham-VT rats (34/36 × 100% = 94%) survived this period. The cause of death for rats was due to general anaesthesia, and these were replaced subsequently. All rats achieved fracture healing.

Plain radiograph for fracture healing. All rats achieved healing at six weeks. Quantitative analysis revealed that the mean relative radiopacity for OVX-VT at 0.62 (SD 0.03) was significantly higher compared to OVX at 0.52 (SD 0.03) ($p < 0.001$) on week 2. Furthermore, mean relative radiopacity for Sham-VT at 0.67 (SD 0.03) was significantly higher compared to Sham at 0.60 (SD 0.02) ($p = 0.020$) on week 2. No other significant differences were observed (Figure 1a).

Micro-CT. Quantitative analysis showed that there was a significant increase of BV/TV ($p = 0.020$) at day 3 for OVX-VT compared to OVX (Figure 1b). There was also significantly higher BV/TV for Sham-VT and Sham compared with OVX-VT ($p = 0.010$) and OVX ($p < 0.001$), respectively, at day 3. At week 6, BV/TV for Sham-VT was significantly higher than that for Sham ($p = 0.030$). Also, Sham-VT was significantly higher than OVX-VT at week 6 ($p = 0.010$).

As for BV, at day 3 and week 1, Sham and Sham-VT were significantly higher compared with OVX ($p < 0.001$) and OVX-VT ($p < 0.001$), respectively. At day 42, BV was found to be significantly higher for Sham-VT compared with Sham ($p = 0.010$). Sham-VT was significantly higher than OVX-VT at day 42 ($p = 0.020$).

TV was found to be significantly higher at day 3 for Sham and Sham-VT compared with OVX ($p < 0.001$) and OVX-VT ($p < 0.001$), respectively. At week 1, TV was also significantly higher for Sham and Sham-VT compared with OVX ($p < 0.001$) and OVX-VT ($p < 0.001$), respectively.

As for trabecular number (Tb.N), Sham was significantly higher than OVX at day 3 ($p = 0.010$). At week 1, Sham-VT was significantly higher compared to OVX-VT ($p = 0.030$). OVX and OVX-VT were also significantly lower compared to Sham ($p = 0.010$) and Sham-VT ($p = 0.030$) at day 14, respectively. This is also reflected in trabecular separation (Tb.Sp), where at day 3 Sham-VT and Sham were significantly lower than OVX-VT ($p = 0.010$) and OVX ($p < 0.001$), respectively. At week 1, Tb.Sp was significantly lower for OVX-VT compared with Sham-VT ($p = 0.030$). At day 14, Tb.Sp was also significantly lower for OVX compared with Sham ($p = 0.020$). At week 6, Sham-VT was significantly lower compared to Sham ($p = 0.020$).

Fibrinolysis cytokine expression in fracture callus by histomorphometry and immunohistochemistry. Martius Scarlet Blue staining revealed a significant decrease of mean fibrin content in the callus in OVX-VT at 2.50% (SD 0.52%) compared with OVX at 10.6% (SD 4.22%) on day 3 ($p = 0.020$). There was also a lower mean fibrin content in Sham-VT at 2.05% (SD 0.73%) as compared with Sham at 6.99% (SD 1.76%) on day 3 Figures 2a and c. Immunohistochemistry of tPA at the fracture callus showed a significantly lower mean amount for OVX-VT at 24.7% (SD 2.46%) compared with OVX at 47.4% (SD 1.11%) on day 3 ($p < 0.001$). Mean tPA for OVX-VT was also significantly lower compared to Sham-VT on day 3 ($p = 0.020$; Figures 2b and c). No significance was seen over PAI-1. Mean VEGF could be identified to be significantly higher for Sham-VT at 13.8% (SD 2.44%) as compared to Sham at 6.90% (SD 1.33%) on week 1 ($p = 0.010$; Figure 2c). As for OVX-VT, mean VEGF was also higher at 4.53% (SD 1.70%) as compared to OVX at 0.86% (SD 0.47%) at week 1. No significance was identified at day 3 (Figure 3).

Fibrinolysis cytokines expression in muscle. Mean tPA from muscle was significantly higher for OVX-VT at 0.64 ng/ml (SD 0.19) as compared to OVX at 0.15 ng/ml (SD 0.05) ($p = 0.020$) on day 3. Furthermore, mean tPA for Sham-VT was also significantly higher at 0.52 ng/ml (SD 0.023) as compared to Sham at 0.09 ng/ml (SD 0.012) ($p = 0.040$) on day 3. As for mean PAI-1, Sham-VT was significantly lower at 25,408 pg/ml (SD 42,034) as compared to Sham at 126,372 pg/ml (SD 126,452) ($p = 0.020$). The trend could also be seen for OVX-VT, whose mean PAI-1 was lower at 1,333.9 pg/ml (SD 823.6) as compared to OVX at 41,428.6 pg/ml (SD 33921.0) on day 3.

Fibrinolysis cytokines in serum. Mean serum PAI-1 was significantly lower for Sham-VT compared to Sham at day 3 ($p < 0.001$). Although not significant, the trend also shows that mean serum PAI-1 for OVX-VT was lower compared to OVX. No significant differences were seen in mean serum tPA for all four groups at each timepoint.

Mechanical testing. Mechanical testing revealed that the mean energy to failure was significantly higher for OVX-VT at 37.6 N mm (SD 8.4) compared with OVX at 5.76 N mm (SD 7.1) ($p = 0.010$) on week 2. The mean energy to failure for Sham-VT was also significantly higher at 39.1 N mm (SD 13.6) compared with Sham at 10.9 N mm (SD 5.0) on week 2 ($p = 0.010$). Furthermore, on week

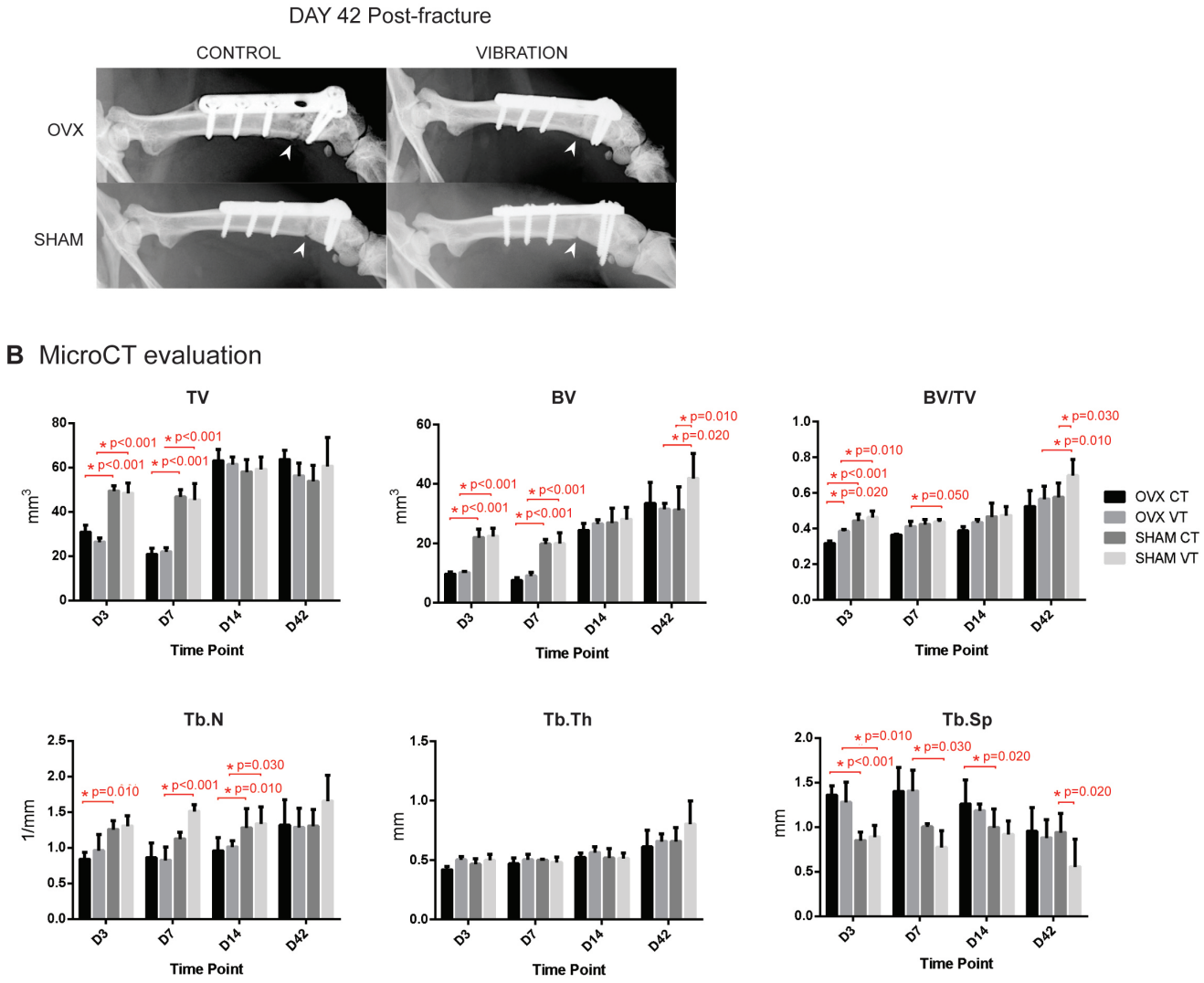

Fig. 1

a) Radiological healing of metaphyseal fracture in Sprague-Dawley rats at Day 42, anteroposterior view. Accelerated healing with increased radiopacity can be seen for the vibration groups. b) Micro-CT evaluation showed a significant increase of bone volume fraction (BV/TV) for ovariectomized with low-magnitude high-frequency vibration (LMHFV) (OVX-VT) compared to ovariectomized-control (OVX-CT), and Sham with LMHFV (Sham-VT) and Sham-control (Sham-CT) compared with OVX-VT and OVX-CT at day 3. *p < 0.05. BV, bone volume; OVX, ovariectomized; Tb.N, trabecular number; Tb.Th, trabecular thickness; Tb.Sp, trabecular separation; TV, tissue volume. One-way analysis of variance with post-hoc Bonferroni test used at each timepoint.

6, mean energy to failure for OVX-VT at 71.9 N mm (SD 30.7) was significantly higher compared to OVX at 17.7 N mm (SD 11.5) (p = 0.030). As for mean stiffness, Sham at 16.7 N/mm (SD 6.6) was significantly higher compared to OVX at 2.42 N/mm (SD 0.8) on week 2 (p = 0.040). The mean stiffness of OVX-VT and Sham-VT was also higher compared to OVX and Sham, respectively, at week 2 and week 6, although significance had not been reached. As for mean ultimate force, Sham at 22.9 N (SD 5.1) was significantly higher compared to OVX at 4.59 N (SD 4.2) on week 2 (p = 0.050). The mean ultimate force of OVX-VT was also higher compared to OVX at week 2 and week 6 (Figure 4).

Discussion

Impaired fibrinolysis is linked to osteoporosis.[12] Studies have shown that oestrogen deficiency is strongly associated with decreased fibrinolytic potential and with impaired fracture healing.[25] Both tPA and plasminogen activator inhibitor-1 (PAI-1) are expressed in human skeletal muscle and endothelial cells.[26] Bone and muscle are intimately linked and these two regions are therefore key areas for investigation of the relationship between vibration therapy and the impact on fibrinolysis. Our results have shown that the fibrinolysis pathway was accelerated by LMHFV shown by multiple markers at day 3, thereby enhancing fracture healing. There was a significant increase of tPA at day 3 for both vibration

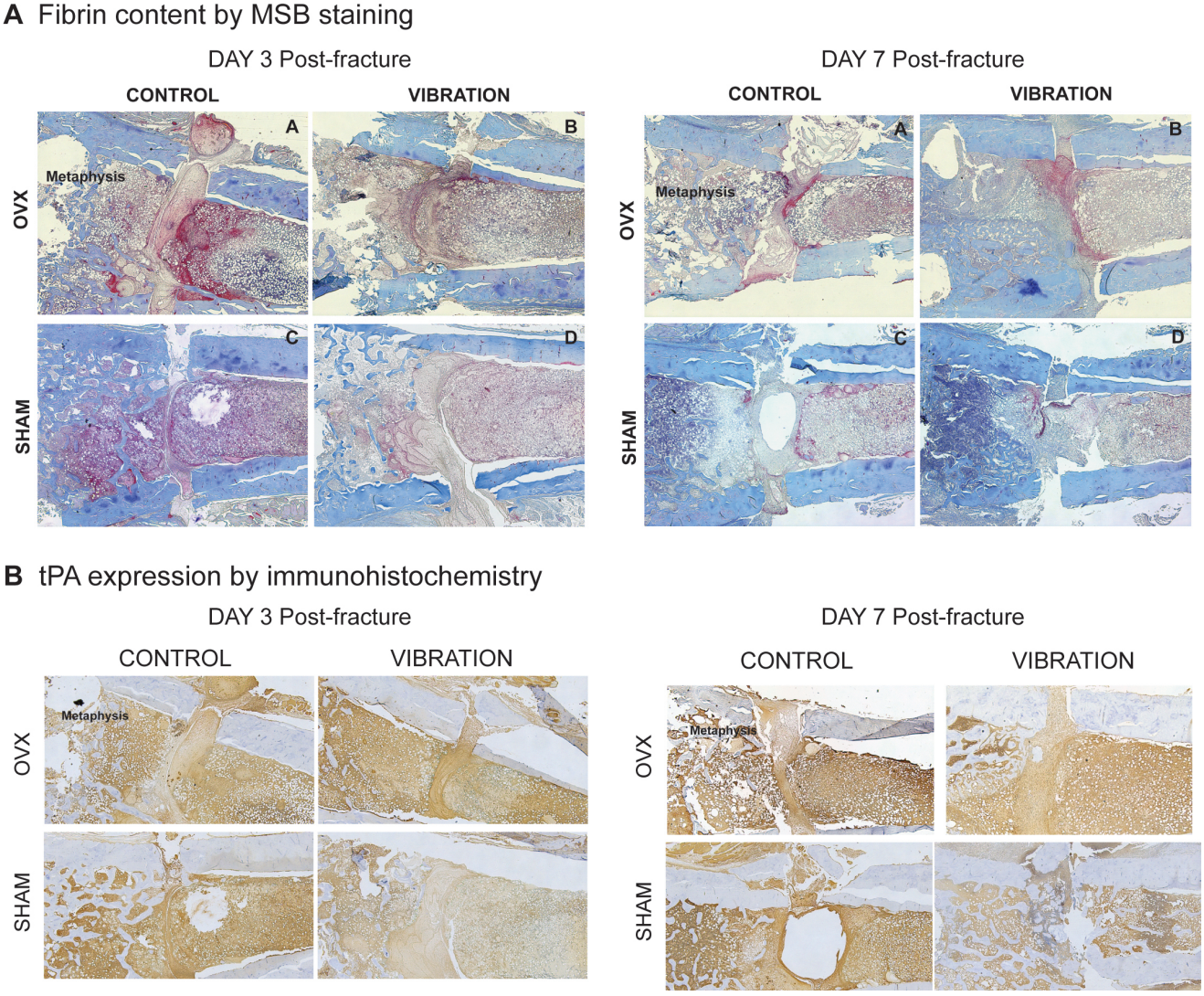

Fig. 2

a) Martius Scarlet Blue (MSB) staining for fibrin content shows that vibration groups have less haematoma at day 3 post-fracture compared to respective control groups at 5× magnification. At day 7 post-fracture, there are no significant differences. b) Immunohistochemistry (IHC) staining for tissue plasminogen activator (tPA) expression, with less for vibration groups at day 3 post-fracture as it is consumed for fibrinolysis. c) Graphs showing fibrin content, tPA, and plasminogen activator inhibitor-1 (PAI-1). *p < 0.05, one-way analysis of variance with post-hoc Bonferroni test. LMHFV, low-magnitude high frequency vibration; OVX-CT, ovariectomized-control; OVX-VT, ovariectomized with LMHFV; Sham-CT, Sham-control; Sham-VT, Sham with LMHFV.

treatment groups. At the fracture site, tPA binds with plasminogen to form plasmin and therefore leads to a significant consumption in tPa for OVX-VT due to this process.

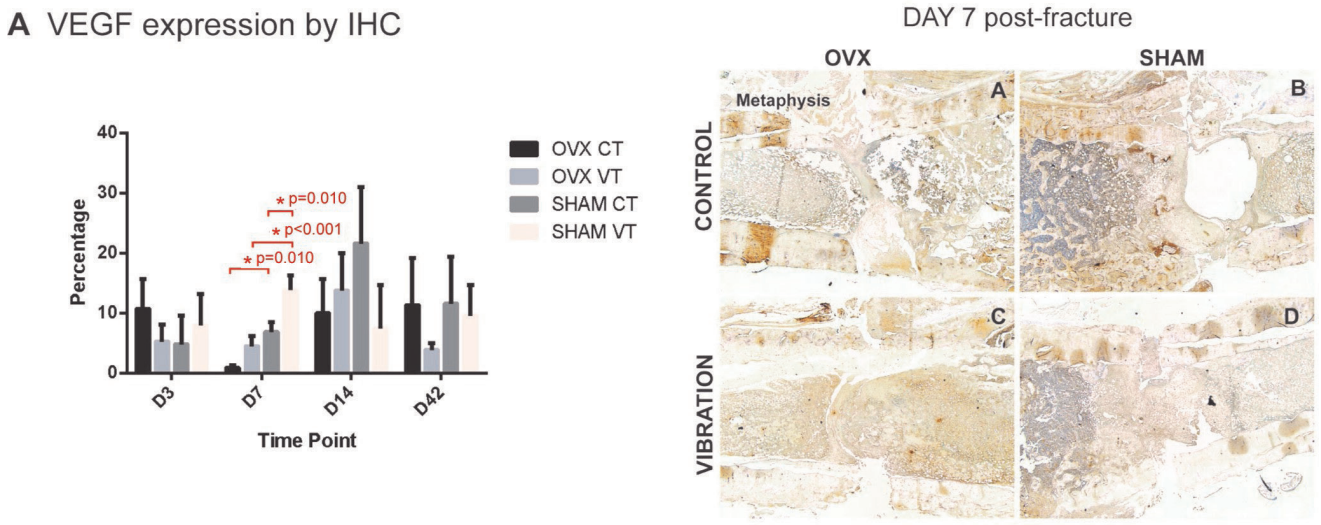

Fig. 3

a) Vascular endothelial growth factor (VEGF) expression shown to be higher for vibration groups at day 7 post-fracture. b) Representative histology of VEGF expression detected by immunohistochemistry (IHC) at day 7 post-fracture, at 5× magnification. *p < 0.05, one-way analysis of variance with Bonferroni test. OVX-CT, ovariectomized-control; OVX-VT, ovariectomized with low-magnitude high-frequency vibration (LMHFV); Sham-CT, Sham-control; Sham-VT, Sham with LMHFV.

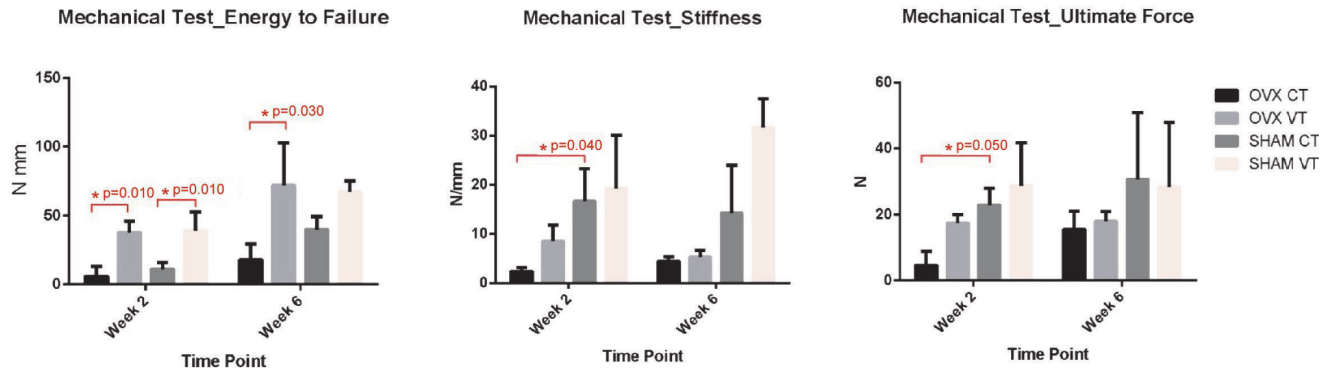

Fig. 4

Results of mechanical testing showed a significantly higher mean energy to failure for ovariectomized with low-magnitude high-frequency vibration (LMHFV) (OVX-VT) than ovariectomized-control (OVX-CT) at week 2 and week 6, and Sham with LMHFV (Sham-VT) than Sham-control (Sham-CT) at week 2. Statisical significance was also detected in stiffness and ultimate force between the OVX-CT and Sham-CT groups. *p < 0.050, one-way analysis of variance with post-hoc Bonferroni test.

The significant decrease of PAI-1 at day 3 for OVX-VT at the fracture callus also showed that the fibrinolytic profile was improved with LMHFV. Systemically, serum PAI-1 was also decreased in the LMHFV groups at day 3. More importantly, fibrin content from MSB staining demonstrates the significant decrease at day 3 for OVX-VT and the same trend for Sham-VT. These results suggest that LMHFV is effective in both normal and osteoporotic bone during fibrinolysis. It can also be observed that immunohistochemical staining of tPA at the fracture callus for osteoporotic bone was significantly lower compared to normal bone, and this demonstrates an accelerated consumption of tPA during fibrinolysis (Figure 5).

Following haematoma clot breakdown, angiogenesis occurs and our results show VEGF to be higher at week 1 for Sham-VT and OVX-VT as compared to Sham and OVX, respectively.[10,11] These observations are consistent and supported by our previous study revealing that vibration therapy could enhance neovascularization of the fracture site,[27] while demonstrating the importance of the preceding fibrinolysis process. During fracture healing, fibrin causes failure of vessels to invade through bone ends and therefore degradation of the clot is an important process for angiogenesis.[10] We observed a significantly increased BV/TV for OVX-VT compared with OVX, and Sham compared with OVX at day 3. These results suggest that by accelerating the fibrinolysis, LMHFV can promote the fracture healing at an early stage. More importantly, results showed only a 3.8% difference for energy to failure between OVX-VT and Sham-VT at week 2, demonstrating the effectiveness

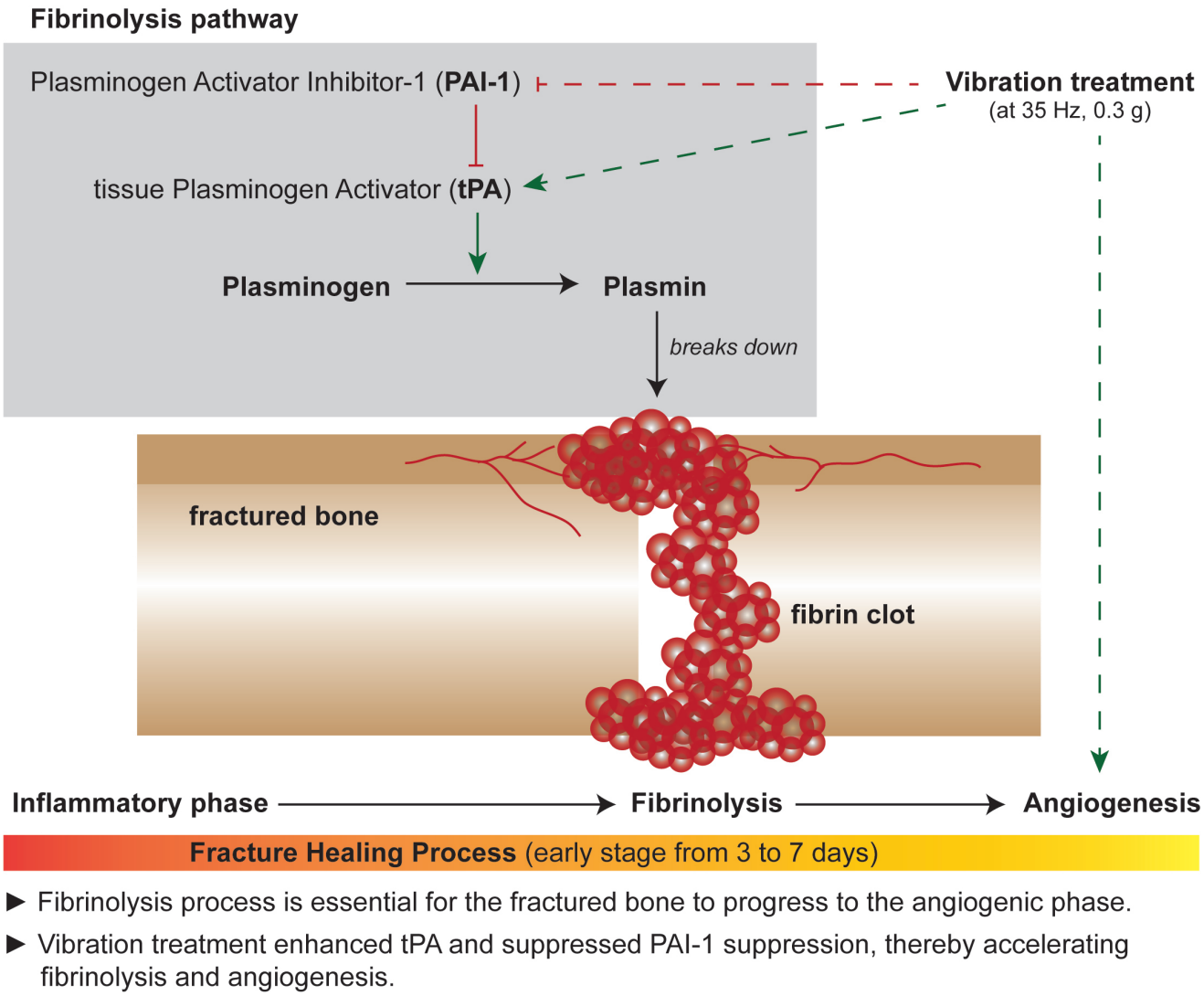

Fig. 5

Illustration for the early fracture healing process involving fibrinolysis.

of vibration therapy in improving mechanical strength. Studies have shown that osteoporotic bone responds as effectively to mechanical stimulation as normal bone.[28] Due to accelerated fibrinolysis, fracture healing occurs at a faster pace with LMHFV and this is reflected at week 6 with higher BV/TV and energy to failure when approaching the remodelling phase.[11]

Metaphyseal fracture healing is accelerated by LMHFV in terms of x-rays, micro-CT, and biomechanical strength. Our current study shows the healing of metaphyseal fractures to be a combination of intramembranous ossification with trabecular bone formation. No external callus was observed in our histological slides. This also echoes the clinical situation where external callus is seldom observed in metaphyseal fracture healing. Trabecular bone formation is an important marker for testing and assessing future interventions or therapeutics in enhancing the healing of osteoporotic fracture, which has been shown in our study. More importantly, the significant findings at day 3 and week 2 for vibration therapy in our results suggest that the enhancement of osteoporotic fracture healing by LMHFV occurs at the early stages that include the inflammatory responses.[29] It is clear that LMHFV enhances metaphyseal fracture healing, and micro-CT results also show that Sham-VT has significantly higher BV compared with OVX-VT in the early and late stages. As fracture healing is closely related to bone, this could explain the improvement of fibrinolytic factors at the local fracture region. This is the first study showing evidence that vibration therapy enhances fibrinolysis and accelerates osteoporotic metaphyseal fracture healing. Previous studies have focussed on the use of the osteoporotic diaphyseal fracture animal model, which has been suggested to not be clinically relevant as most osteoporotic fractures occur at the metaphysis.[30]

The current limitation of this study is that animal models cannot fully simulate humans and need translation to patients. Despite accumulating evidence supporting the therapeutic effect of LMHFV treatment on enhancing fracture healing from preclinical studies, large-scale randomized controlled trials are still warranted to validate these findings for clinical application.

With the novel finding that fibrinolysis pathway was accelerated by LMHFV, our study provides a more comprehensive understanding of the effect of LMHFV on bone healing. Nevertheless, LMHFV can promote fracture healing through multiple pathways, including enhancing mesenchymal stem cell recruitment, angiogenesis, callus formation, and mineralization.[31] Furthermore, currently the Food and Drug Administration (FDA) recommends that osteoporotic studies be evaluated by the OVX rat and a larger OVX non-rodent species. Thus, further studies may be required to confirm our findings.

Impaired fracture healing and fibrinolytic activity is commonly associated with comorbidities including obesity, diabetes, smoking, and advanced age.[10,11] With the ageing population, further studies that target fibrinolysis to improve fracture healing in patients at risk are warranted. To our knowledge, this is the first study to enhance fracture healing through this molecular pathway. Although the haematoma clot plays a major role in the initial haemostasis of a fracture, acting upon the fibrinolytic system has proven to be safe in our study. No clinical complications or excess bleeding were identified. In conclusion, metaphyseal fracture healing is enhanced by LMHFV, and one of the important molecular pathways it acts on is fibrinolysis. LMHFV is a promising intervention for osteoporotic metaphyseal fracture healing. Given the safe application of LMHFV, future translation may provide a significant impact to our fragility fracture patients.

References

1. **Solomon DH**, **Patrick AR**, **Schousboe J**, **Losina E**. The potential economic benefits of improved postfracture care: a cost-effectiveness analysis of a fracture liaison service in the US health-care system. *J Bone Miner Res*. 2014;29(7):1667–1674.
2. **Rachner TD**, **Khosla S**, **Hofbauer LC**. Osteoporosis: now and the future. *Lancet*. 2011;377(9773):1276–1287.
3. **Wong RMY**, **Ho WT**, **Wai LS**, **et al**. Fragility fractures and imminent fracture risk in Hong Kong: one of the cities with longest life expectancies. *Arch Osteoporos*. 2019;14(1):104.
4. **Alt V**, **Thormann U**, **Ray S**, **et al**. A new metaphyseal bone defect model in osteoporotic rats to study biomaterials for the enhancement of bone healing in osteoporotic fractures. *Acta Biomater*. 2013;9(6):7035–7042.
5. **Wong RMY**, **Law SW**, **Lee KB**, **Chow SKH**, **Cheung WH**. Secondary prevention of fragility fractures: instrumental role of a fracture liaison service to tackle the risk of imminent fracture. *Hong Kong Med J*. 2019;25(3):235–242.
6. **Wong RMY**, **Choy MHV**, **Li MCM**, **et al**. A systematic review of current osteoporotic metaphyseal fracture animal models. *Bone Joint Res*. 2018;7(1):6–11.
7. **Wang C**, **Zheng G-F**, **Xu X-F**. Microrna-186 improves fracture healing through activating the bone morphogenetic protein signalling pathway by inhibiting Smad6 in a mouse model of femoral fracture: an animal study. *Bone Joint Res*. 2019;8(11):550–562.
8. **Peng X**, **Wu X**, **Zhang J**, **Zhang G**, **Li G**, **Pan X**. The role of CKIP-1 in osteoporosis development and treatment. *Bone Joint Res*. 2018;7(2):173–178.
9. **Winkler T**, **Sass FA**, **Duda GN**, **Schmidt-Bleek K**. A review of biomaterials in bone defect healing, remaining shortcomings and future opportunities for bone tissue engineering: the unsolved challenge. *Bone Joint Res*. 2018;7(3):232–243.
10. **Yuasa M**, **Mignemi NA**, **Nyman JS**, **et al**. Fibrinolysis is essential for fracture repair and prevention of heterotopic ossification. *J Clin Invest*. 2015;125(8):3117–3131.
11. **O'Keefe RJ**. Fibrinolysis as a target to enhance fracture healing. *N Engl J Med*. 2015;373(18):1776–1778.
12. **Cole HA**, **Ohba T**, **Nyman JS**, **et al**. Fibrin accumulation secondary to loss of plasmin-mediated fibrinolysis drives inflammatory osteoporosis in mice. *Arthritis Rheumatol*. 2014;66(8):2222–2233.
13. **Gebara OC**, **Mittleman MA**, **Sutherland P**, **et al**. Association between increased estrogen status and increased fibrinolytic potential in the Framingham offspring study. *Circulation*. 1995;91(7):1952–1958.
14. **Lindoff C**, **Petersson F**, **Lecander I**, **Martinsson G**, **Åstedt B**. Passage of the menopause is followed by haemostatic changes. *Maturitas*. 1993;17(1):17–22.
15. **Hsu W-B**, **Hsu W-H**, **Hung J-S**, **Shen W-J**, **Hsu RW-W**. Transcriptome analysis of osteoblasts in an ovariectomized mouse model in response to physical exercise. *Bone Joint Res*. 2018;7(11):601–608.
16. **Qin J**, **Chow SK-H**, **Guo A**, **Wong W-N**, **Leung K-S**, **Cheung W-H**. Low magnitude high frequency vibration accelerated cartilage degeneration but improved epiphyseal bone formation in anterior cruciate ligament transect induced osteoarthritis rat model. *Osteoarthritis Cartilage*. 2014;22(7):1061–1067.
17. **Leung KS**, **Shi HF**, **Cheung WH**, **et al**. Low-magnitude high-frequency vibration accelerates callus formation, mineralization, and fracture healing in rats. *J Orthop Res*. 2009;27(4):458–465.
18. **Ghazalian F**, **Hakemi L**, **Pourkazemi L**, **Akhoond M**. Effects of whole-body vibration training on fibrinolytic and coagulative factors in healthy young men. *J Res Med Sci*. 2014;19(10):982–986.
19. **Wong RM**, **Thormann U**, **Choy MH**, **et al**. A metaphyseal fracture rat model for mechanistic studies of osteoporotic bone healing. *Eur Cell Mater*. 2019;37:420–430.
20. **Shi H-F**, **Cheung W-H**, **Qin L**, **Leung AH-C**, **Leung K-S**. Low-magnitude high-frequency vibration treatment augments fracture healing in ovariectomy-induced osteoporotic bone. *Bone*. 2010;46(5):1299–1305.
21. **Wang X**, **Luo Y**, **Masci PP**, **Crawford R**, **Xiao Y**. Influence of Interleukin-1 Beta on Platelet-Poor Plasma Clot Formation: A Potential Impact on Early Bone Healing. *PLoS One*. 2016;11(2):e0149775.
22. **Chow DH-K**, **Leung K-S**, **Qin L**, **Leung AH-C**, **Cheung W-H**. Low-magnitude high-frequency vibration (LMHFV) enhances bone remodeling in osteoporotic rat femoral fracture healing. *J Orthop Res*. 2011;29(5):746–752.
23. **Sun KT**, **Leung KS**, **Siu PMF**, **Qin L**, **Cheung WH**. Differential effects of low-magnitude high-frequency vibration on reloading hind-limb soleus and gastrocnemius medialis muscles in 28-day tail-suspended rats. *J Musculoskelet Neuronal Interact*. 2015;15(4):316–324.
24. **Leung KS**, **Siu WS**, **Li SF**, **et al**. Anin vitro optimized injectable calcium phosphate cement for augmenting screw fixation in osteopenic goats. *J Biomed Mater Res B Appl Biomater*. 2006;78B(1):153–160.
25. **Chow SKH**, **Leung KS**, **Qin J**, **et al**. Mechanical stimulation enhanced estrogen receptor expression and callus formation in diaphyseal long bone fracture healing in ovariectomy-induced osteoporotic rats. *Osteoporos Int*. 2016;27(10):2989–3000.
26. **Francis RM**, **Romeyn CL**, **Coughlin AM**, **Nagelkirk PR**, **Womack CJ**, **Lemmer JT**. Age and aerobic training status effects on plasma and skeletal muscle tPA and PAI-1. *Eur J Appl Physiol*. 2014;114(6):1229–1238.
27. **Cheung W-H**, **Sun M-H**, **Zheng Y-P**, **et al**. Stimulated angiogenesis for fracture healing augmented by low-magnitude, high-frequency vibration in a rat model-evaluation of pulsed-wave Doppler, 3-D power Doppler ultrasonography and micro-CT microangiography. *Ultrasound Med Biol*. 2012;38(12):2120–2129.
28. **Cheung WH**, **Miclau T**, **Chow SK-H**, **Yang FF**, **Alt V**. Fracture healing in osteoporotic bone. *Injury*. 2016;47 Suppl 2(Suppl 2):S21–S26.
29. **Chow SK-H**, **Chim Y-N**, **Wang J**, **et al**. Vibration treatment modulates macrophage polarisation and enhances early inflammatory response in oestrogen-deficient osteoporotic-fracture healing. *Eur Cell Mater*. 2019;38:228–245.
30. **Wong RMY**, **Choy MHV**, **Li MCM**, **et al**. A systematic review of current osteoporotic metaphyseal fracture animal models. *Bone Joint Res*. 2018;7(1):6–11.
31. **Wang J**, **Leung KS**, **Chow SK**, **Cheung WH**. The effect of whole body vibration on fracture healing - a systematic review. *Eur Cell Mater*. 2017;34:108–127.

Author information:
- R. M. Y. Wong, MBChB, PhD, Clinical Assistant Professor
- V. M. H. Choy, PhD, PhD Candidate

- J. Li, MMed, PhD Candidate
- T. K. Li, BHSc, Research Assistant
- Y. N. Chim, PhD, Postdoctoral Research Fellow
- M. C. M. Li, Research Assistant
- J. C. Y. Cheng, MBBS, MD, Emeritus Professor
- K-S. Leung, MBBS, MD, Emeritus Professor
- S. K-H. Chow, PhD, Research Assistant Professor
- W. H. Cheung, PhD, Associate Professor

Department of Orthopaedics and Traumatology, Prince of Wales Hospital, The Chinese University of Hong Kong, Hong Kong, Hong Kong.

Author contributions:

- R. M. Y. Wong: Analyzed the data, Performed the research, Wrote the paper.
- V. M. H. Choy: Performed the research.
- J. Li: Wrote the paper.
- T. K. Li: Performed the research.
- Y. N. Chim: Performed the research.
- M. C. M. Li: Performed the research.
- J. C. Y. Cheng: Designed the research, Analyzed the data.
- K-S. Leung: Designed the research.
- S. K-H. Chow: Designed the research, Analyzed the data, Wrote the paper.
- W. H. Cheung: Designed the research, Wrote the paper.

Funding statement:

- This study was supported by the Health and Medical Research Fund, Food and Health Bureau, Hong Kong SAR Government (Reference no. 04152406), Hong Kong Research Grants Council Early Career Scheme (Reference no. 24108519), and Asian Association for Dynamic Osteosynthesis (Ref: AADO-RF2016-2Y). No benefits in any form have been received or will be received from a commercial party related directly or indirectly to the subject of this article.

Acknowledgements:

- The authors would like to acknowledge W-T. Ho (Department of Orthopaedics and Traumatology, The Chinese University of Hong Kong) for her contributions.